Gas chromatographic investigation of the competition between mass transfer and kinetics on a solid catalyst

V. Loukopoulos, D. Gavril, G. Karaiskakis, N.A. Katsanos*

Department of Chemistry, University of Patras, 26504 Patras, Greece

Received 23 July 2004; received in revised form 29 September 2004; accepted 30 September 2004

Abstract

The reversed-flow gas chromatography (RF-GC) method is used to investigate the competition between mass transfer and kinetics in heterogeneous catalysis. The well-studied dissociative adsorption of carbon monoxide over a silica supported rhodium catalyst at various temperatures is used as model system. The Thiele-type modulus Φ_s and the effectiveness factor η are calculated for both adsorbate (CO) and product (CO_2), from the experimental chromatographic peaks. The values experimentally found are similar to those predicted theoretically and give interesting information for the mechanism of the interaction of carbon monoxide with the catalyst studied.
© 2004 Published by Elsevier B.V.

Keywords: Inverse gas chromatography; Physicochemical measurements; Mass transfer; Kinetics; Rhodium; Heterogeneous catalysis

1. Introduction

The use of catalysts has given solutions in many aspects of technological and environmental interest. In the majority of the heterogeneous catalysts, the active phases (usually noble metals or metal oxides) are supported over a porous solid material such as silica, alumina, etc. The performance of such a catalyst is greatly affected from the competition between mass transfer taking place in the pores of the supporting material and the kinetics of the adsorbate–adsorbent interaction. Mass transfer phenomena usually prevail at lower temperatures, since diffusion in solids is a temperature-activated process. On the other hand, gas–solid chromatography is also closely related to diffusion in solids and chemical kinetics. In heterogeneous catalysis, the competition between kinetics and mass transfer is usually indirectly investigated, e.g., from the temperature variation of the catalytic activity. The development of a gas chromatographic methodology capable to directly determine which one of the above-mentioned processes prevails in a particular tem-

perature is important for both heterogeneous catalysis and chromatography.

Various forms of gas chromatography have been used for studying surface catalyzed transformation of substances, starting from the work of Bassett and Habgood [1] who used classical elution chromatography, and ending to the situation used in the present work, which is a special version of inverse gas chromatography. A recent review on catalytic studies by gas chromatography has been published [2]. It shortly describes adsorption physicochemical quantities and catalytic properties. The methods for the determination of rate constants from experimental chromatograms are related to the peak area (zeroth statistical moment), to higher moments or to fitting procedures using numerical solutions of the model partial differential equations. The latter can be used in principle without any limitation, but the evaluations are still cumbersome, even with large computers. Their importance will probably increase in the future, numerical algorithms especially designed for the solution of chromatography models having been compared and discussed [3].

In all above and other situations, however, the method has remained a pure chromatographic one, being simply termed

---

* Corresponding author. Tel.: +30 2610 997144; fax: +30 2610 997144.
  E-mail address: rita@chemistry.upatras.gr (N.A. Katsanos).

"inverse gas chromatography" since the stationary phase is the object of the investigation. It is an integral method of kinetic measurements, since the chromatographic band appears as a result of integrating the various physical and chemical phenomena are taking place by passing the reacting system through the whole column, and exposing only the integral result in the form of an elution band. What details are hidden under this band is difficult, if not impossible, to see, particularly the heterogeneity effects of the solid catalyst. It rather resembles a kinetic experiment in a closed glass vessel, analyzing the resulting mixture when a considerable time period has passed. Of course, some corrections can be made by an extrapolation to infinite dilution and zero carrier gas flow-rate, as explained in a book [4]. These are, however, only corrections and not experimental facts.

In order that a *differential method* is employed to measure rates of physicochemical phenomena entering the area of time-resolved chemistry, the traditional chromatographic procedure has to be abandoned, without abandoning the chromatographs. The first such idea occurred to Phillips in 1967 [5], who stopped the carrier gas flow, i.e., the chromatography, and then restored it after a short time period, repeatedly. The differential rate of a catalytic reaction is measured taking place on the stationary phase of the column. Probably, the main drawback of the method is that it continuously switches the system under study from a flow dynamic one to a static system and vice versa.

There is another way to remove the phenomenon of chromatography from our experiments, retaining all chromatographic components (carrier gas, injectors, detectors, integrators, etc.), by simply placing the solid material (adsorbents, catalysts, etc.) *perpendicular* to the direction of the carrier gas flow, which runs at a distance above it, but not through it. The method is termed reversed-flow gas chromatography (RF-GC), because it samples the reacting system from time to time by simply reversing the direction of the carrier gas flow (for 2–60 s) and then returning it to its original direction. This procedure samples the gaseous phase above the solid surface, the sampling appearing in the detector as sharp very narrow peaks, like those of Fig. 2 in the review [2]. Each "sample peak" like those is a differential sampling with respect to time referring only at the time when the reversal was made, and integrating the concentrations only within the time period of the few seconds that the reversed flow lasted (2–60 s).

If the sample peaks described above are mixtures of more than one substance, they can be analyzed by another classical separation column, placed before the detector, as shown in Fig. 3 of ref. [2]. A typical example is the reactant A and the product B of the phenomenon A → B, like dehydration of alcohols [6], catalytic deamination [7], catalytic cracking [8], hydrodesulfurization reactions [9], methanation of carbon monoxide [10], etc. [11]. However, apart from reaction rate constant, adsorption/desorption rate constants and overall adsorption isotherms, no other physicochemical

quantity was measured by the reversed-flow method until 1999, when time distribution of adsorption energies, local monolayer capacities and local isotherms [12], probability density functions for adsorption energies [13], surface diffusion coefficients [14], lateral molecular interaction on the solid surface [15], adsorption rates with lateral interactions [16], and surface energy [17], all the above been measured on heterogeneous surfaces, as a function of the observation time.

In this domain belongs the object of the present work namely, the presentation of a novel aspect of RF-GC for the investigation of the competition between mass transfer and kinetics. The well-studied dissociative adsorption (disproportionation) of CO to CO_2 over a typical solid catalyst of pure rhodium supported on SiO_2, at three different temperatures is used as a model system.

Moreover, another thing never done before, as far as we know, is the simultaneous detection and measurement of both reactant CO and product CO_2 at various chosen times, and the calculation from them of all the physicochemical quantities mentioned before, pertaining to the heterogeneous surface of the catalyst.

2. Experimental

The experimental set-up of the RF-GC method can be found in previous work [2,12,13].

A small volume (1 cm^3 at atmospheric pressure) of the CO adsorbate gas (from Linde A.G., Greece, 99.97% pure) was injected at the end of the solid bed [0.15 g of 3% (w/w) rhodium supported on silica gel 60 of Merck, $d < 0.063$ mm, 70–230 mesh ASTM]. The diffusion column had a length of $L_1 = 70.0$ cm, and was connected to the solid bed $L_2 = 1.0$ cm, which contained the catalyst. Both sections had an i.d. of 5.3 mm. The sampling column was $l = l' = 38.0$ cm long and 5.3 mm wide.

The carrier gas (99.999% He from BOC Gases, Greece, dried with silica gel) was running with a flow-rate of 68.2 cm^3 min^{-1}, while a column filled with 7.6 g of silica gel 80–100 mesh from Supelco, of length L' (45 cm × 5.3 mm i.d.) was used for the separation of reactant CO and product CO_2. The separation column L' was connected before the detector. All columns were conditioned by heating them in situ at 743 K, for 20 h, under carrier gas flow. After that, the temperature was regulated at a lower working value, and by means of the valve included in the system the direction of the carrier gas flow through the sampling column was reversed for 5 s every 2 min. Following each flow reversal, two very narrow (2.5 s at half-height) and symmetrical *sample peaks* of CO and CO_2 of considerable heights H (cm) above the continuous signal were recorded. A series (32–38) of such pairs of peaks was obtained, the height of which together with the time t (min) of the corresponding flow-reversal were printed by a C-R6A Shimadzu Chromatopac.

3. Theoretical and calculations

3.1. The reactant carbon monoxide

As regards the mathematical model, and the solution of the system of partial differential equations resulting for the reactant (CO in the present work), these have been recently published more than once [14,16–19]. Only the final result, the meaning of the various symbols, and some intermediate equations are needed for the product CO_2 analysis and are repeated here.

The sample peaks height H resulting from the flow reversals at various times t and printed by the recording system follows Eq. (27) of ref. [16]:

$$H^{1/M} = \sum_{i=1}^{3} A_i \exp(B_i t) = gG \sum_{i=1}^{3} A_i^0 \exp(B_i t) \qquad (1)$$

where M is the response factor of the detector, g is the calibration factor of the detector (height in cm per concentration in $mol\,cm^{-3}$) and G is given by:

$$G = \frac{n_A a_1 a_2}{\dot{V}(a_1 + a_2 + a_2 Q_2)} \qquad (2)$$

n_A being the amount of injected CO (mol), $\dot{V}$ is the volumetric flow-rate of the carrier gas ($cm^3\,min^{-1}$), and

$$a_1 = \frac{2D_z}{L_1^2}; \quad a_2 = \frac{2D_y}{L_2^2}; \quad Q = \frac{2a_y L_2}{a_z L_1} \qquad (3)$$

D_z and D_y denoting the gaseous diffusion coefficient of reactant in volume z and y, respectively, coefficient a_y and a_z being the free cross sectional areas in the y and z coordinate, respectively. The A_i^0, B_i are physicochemical parameters with the following content [16]:

$$A_1^0 = \frac{B_1^2 + kB_1}{(B_1 - B_2)(B_1 - B_3)}; \quad A_2^0 = \frac{B_2^2 + kB_2}{(B_2 - B_1)(B_2 - B_3)};$$

$$A_3^0 = \frac{B_3^2 + kB_3}{(B_3 - B_1)(B_3 - B_2)} \qquad (4)$$

$$-(B_1 + B_2 + B_3) = X_1 = \frac{\alpha_1 \alpha_2}{\alpha_1 + \alpha_2 + \alpha_2 Q} + k \qquad (5)$$

$$B_1 B_2 + B_1 B_3 + B_2 B_3 = Y_1 = \frac{\alpha_1 \alpha_2 k + (\alpha_1 + \alpha_2 Q)k_1 k_R}{\alpha_1 + \alpha_2 + \alpha_2 Q} \qquad (6)$$

$$-B_1 B_2 B_3 = Z_1 = \frac{\alpha_1 + \alpha_2 Q}{\alpha_1 + \alpha_2 + \alpha_2 Q} k_1 k_2 k_R \qquad (7)$$

The k_1, k_2 and k_R are the rate constants for the adsorption isotherm, the first or pseudo first-order surface reaction of CO to CO_2, and the adsorption/desorption on the bulk solid, respectively, while $k = k_2 + k_R$.

The value of k is found from Eq. (4) by combining any two of them. Then, using this value in Eq. (5), one easily calculates a_2 and then D_y by Eq. (3). From Eq. (6) one finds $k_1 k_R$, and from Eq. (7) $k_1 k_2 k_R$. Division of the latter two gives k_2. Subtraction of that from k already found gives k_R, and finally dividing $k_1 k_R$ by that results in k_1. Thus, D_y, k_1, k_2, k_R are all obtained directly from the parameters A_1, A_2, A_3 and B_1, B_2, B_3 of Eq. (1), as determined by non-linear least squares fitting of the experimental pairs H, t to that equation. Relevant PC programs for these calculations have recently been published [16–19].

Having carried out the previous calculations, all other physicochemical quantities pertaining to heterogeneous surfaces and recently summarized [20] can easily be found, namely, time distribution of adsorption energies, local monolayer capacities, and local isotherms [12], probability density function for the adsorption energy [13], lateral molecular interaction on the surfaces [15], surface diffusion coefficients [14], adsorption rates with lateral interactions [16], surface energy [21], etc.

3.2. The product carbon dioxide

The mathematical model describing the product of a chemical reaction on the chromatographic material (catalyst) is somehow different from that of the reactant for the following reasons: (a) the product is not injected initially onto the solid bed as was done with the reactant; (b) the product is continuously produced from the reactant while all experimental manipulations are conducted; (c) the mathematical equations include a surface concentration of the reactant continuously changing with place and time in the solid bed.

The rate of change of the product CO_2 in the empty of solid section z is:

$$\frac{\partial c_{zp}}{\partial t} = D_{zp} \cdot \frac{\partial^2 c_{zp}}{\partial z^2} \qquad (8)$$

where c_{zp} is the concentration of CO_2 in the gas ($mol\,cm^{-3}$) and D_{zp} its diffusion coefficient in the carrier gas. The Laplace transformation with respect to t (parameter p) of the above equation is taken under the initial condition $c_{zp}(0, z) = 0$. Then, the transformation is doubled with respect to z (parameter s), and after simple algebraic manipulations it is inversed with respect to s giving

$$C_{zp}(L_1) = C_{zp}(0) \cosh q_{1p}z + \frac{C'_{zp}(0)}{q_{1p}} \sinh q_{1p}z \qquad (9)$$

where the capital letter C_{zp} represents the t transformed c_{zp}, $C_{zp}(0)$ refers to $z = 0$, $C'_{zp}(0) = (dC_{zp}/dz)_{z=0}$, and $q_{1p} = \sqrt{p/D_{zp}}$.

Eq. (9) is simplified as before [16] leading to the following result analogous to Eq. (8) there:

$$C_{zp} = \frac{\upsilon C_p(l', p)}{D_{zp} q_{1p}} \sinh q_{1p}z \qquad (10)$$

where υ is the linear flow velocity ($cm\,s^{-1}$) of the carrier gas in the sampling column, and $C_p(l', p)$ the t Laplace trans-

form of the measurable concentration $c_p(l', t)$ of CO_2 in this column.

The next equation is that describing the product CO_2 in the gaseous phase of the section y filled with the catalyst:

$$\frac{\partial c_{yp}}{\partial t} = D_{yp}\frac{\partial^2 c_{yp}}{\partial y^2} + k_{Rp}\frac{a_s}{a_y}(c_{sp} - c_{sp}^*) \tag{11}$$

which is exactly the same as Eq. (2) of ref. [16]. Here c_{yp} is the concentration in the gas phase of region y (mol cm^{-3}), D_{yp} the effective diffusion coefficient in the solid bed (cm^2 s^{-1}), k_{Rp} the rate constant for adsorption/desorption on the bulk solid catalyst (s^{-1}), a_s the amount of the catalyst per unit length of the bed (g cm^{-1}), a_y the free cross sectional area in the bed (cm^2), c_{sp} the adsorbed concentration of the product (mol g^{-1}), and c_{sp}^* its local adsorbed equilibrium concentration on the solid at time t.

The concentration change of the adsorbed CO_2 is described by an equation again analogous to that of the reactant (Eq. (3) of ref. [16]), the only difference being the last term on the right-hand side, now being $+k_2 c_s$ instead of $-k_2 c_s$, the surface concentration c_s being again that of the reactant CO:

$$\frac{\partial c_{sp}}{\partial t} = k_{Rp}(c_{sp}^* - c_{sp}) + k_2 c_s \tag{12}$$

Here k_2 is the rate constant of the reaction for the transformation of CO to CO_2, incorporated already in Section 3.1 for the reactant.

To solve the system of the two partial differential Eqs. (11) and (12), only the isotherm equation of the reactant is required (Eq. (4) of ref. [16]):

$$c_s^* = \frac{a_y}{a_s} \cdot k_1 \int_0^t c_y(\tau)d\tau \tag{13}$$

where c_s^* is the equilibrium concentration on the solid at time t of the reactant, k_1 the isotherm rate constant already calculated in Section 3.1, c_y the gaseous concentration of the reactant and τ a dummy variable for time (s).

The relation between c_s^* of Eq. (13) above and c_s of Eq. (12) is found by writing an equation analogous to Eq. (12) for the reactant:

$$\frac{\partial c_s}{\partial t} = k_R(c_s^* - c_s) - k_2 c_s \tag{14}$$

If one writes an isotherm equation for the product exactly the same with Eq. (13) of the reactant, the system of Eqs. (11)–(14) can be solved obtaining an equation for the product analogous to Eq. (1) of the reactant, the only difference being the range of index i in the summation, which becomes

$i = 1$–5 for the product. The experimental facts for the product, being the pairs H, t of peak height and the respective time, can be used with a PC program similar to that already used for the reactant, but with five exponential terms $A_i \exp(B_i t)$ in Eq. (1). Such a non-linear least squares fitting of the experimental data, however, is not highly acceptable, leading to tremendous errors and a very poor repeatability. This is expected since, proper errors of the final results of k_1, k_R, k_2 and D_y (cf. Table 1) should be based on the principle of propagation of errors involving five values of A_i ($i = 1$–5) of Eq. (1). Only recently, such a calculation was tried with $i = 1$–3, i.e., with six independent variables and their errors in a study of diffusion and adsorption coefficients in porous solids. It was found that the standard error of D_y is about 3%, whereas that of the sum $k_R + k_2$ about 10%. The results are under preparation for publication. For this reason a steady-state approximation for the adsorbed product c_{sp} is adopted in Eq. (12), namely $\partial c_{sp}/\partial t = 0$, physically logical since the adsorbed CO_2 is produced from the adsorbed CO as term $k_2 c_s$ indicates, and disappears when $c_{sp} > c_{sp}^*$ towards the gas phase as Eqs. (12) and (11) show. A similar steady-state approximation has been adopted before [22]. Here, it probably implies that k_{Rp} of Eq. (12) is larger than k_2, but this cannot be tested experimentally, since k_{Rp} cannot be calculated as k_R, given in Table 1 and referring only to the reactant.

As was done with Eq. (8) for the product in the region z of the diffusion column, the time Laplace transforms (parameter p) are taken for Eqs. (11)–(14) with initial conditions

$$c_{yp}(0, y) = c_{sp}(0, y) = c_s(0, y) = 0 \tag{15}$$

with the following results, using capital letters for the transformed functions, and after some rearrangements. From Eq. (11) one obtains

$$\frac{d^2 C_{yp}}{dy^2} = \frac{p}{D_{yp}}C_{yp} - \frac{k_{Rp}}{D_{yp}}\frac{a_s}{a_y}(C_{sp} - C_{sp}^*) \tag{16}$$

From Eq. (12), after a steady state assumption $\partial c_{sp}/\partial t = 0$ for c_{sp}, there results

$$k_{Rp}(C_{sp} - C_{sp}^*) = k_2 C_s \tag{17}$$

From Eq. (13)

$$C_s^* = \frac{a_y}{a_s} \cdot k_1 \cdot \frac{C_y}{p} \tag{18}$$

Table 1
Dynamic adsorption rate constant k_1, adsorption/desorption rate constant k_R, first-order rate constant k_2 of surface production of CO_2 from CO, and total diffusion coefficients in the solid bed for the adsorbate CO (D_y), as well as its dissociation product CO_2 (D_{yp}).

T (K)	k_1 (10^{-4} s^{-1})	k_R (10^{-3} s^{-1})	k_2 (10^{-3} s^{-1})	D_y(10^{-4} cm^2 s^{-1})	D_{yp}(10^{-4} cm^2 s^{-1})
473.2	1.51	3.12	3.64	2.15	1.69
573.2	6.99	0.51	6.83	2.95	5.40
598.2	75.4	0.056	6.02	3.12	2.44

and from Eq. (14) referring to the reactant

$$C_s = \frac{k_R C_s^*}{p + k_R + k_2} \tag{19}$$

the meaning of k_1, k_R and k_2 having being explained in Section 3.1 for the reactant.

Substituting the right-hand side of Eq. (19) for C_s in Eq. (17), and the resulting right-hand side for $k_{Rp}(C_{sp} - C_{sp}^*)$ in Eq. (16), one obtains

$$\frac{d^2 C_{yp}}{dy^2} = \frac{p}{D_{yp}} \cdot C_{yp} - \frac{a_s}{D_{yp} a_y} \cdot \frac{k_R k_2 C_s^*}{p + k_R + k_2} \tag{20}$$

Finally, Eq. (18) being substituted above for C_s^* gives

$$\frac{d^2 C_{yp}}{dy^2} = q_{2p}^2 C_{yp} - \frac{k_1 k_R k_2 C_y}{D_{yp} p(p + k_R + k_2)} \tag{21}$$

where $q_{2p}^2 = p/D_{yp}$

Eq. (21) gives the dependence of the gaseous product CO_2 concentration C_{yp} on the gaseous concentration C_y of the reactant CO, for any time and on any point of the catalyst bed, in terms of three rate constants k_1, k_2, k_R of the reactant, and the effective diffusion coefficient D_{yp} of the product in the bed.

To make the differential Eq. (21) more specific with respect to the length coordinate y and the time t, one must solve it for these two independent variables. It is already an equation transformed with respect to time as regards the two gaseous concentrations c_{yp} and c_y. It remains to transform it with respect to length y (parameter s), then, after some necessary manipulations to take the inverse s transformation, and finally end with the inverse p transformation, to obtain the concentrations of both reactant and product as functions of the experimental time, valid for a specific point of the solid bed ($y = 0$).

The result of the first two procedures is

$$C_{yp} = C_{yp}(0) \cosh q_{2p} y + \frac{C_{yp}'(0)}{q_{2p}} \cdot \sinh q_{2p} y$$
$$- q_r^2 \int_0^y \frac{\sinh q_{2p} w}{q_{2p}} \cdot C_y(y - w) dw \tag{22}$$

where $C_{yp}(0)$ refers to $y = 0$, $C_{yp}'(0) = (dC_{yp}/dy)_{y=0}$,

$$q_r^2 = \frac{k_1 k_R k_2}{D_{yp} p(p + k_R + k_2)} \tag{23}$$

and $q_{2p} = \sqrt{p/D_{yp}}$ as before, whereas the last term of Eq. (22) is a convolution between $\sinh q_{2p} y$ and C_y, i.e., a term belonging to the product and another to the reactant. A usual approximation adopted in similar work [22] is $\sinh qx \approx qx$, i.e., to retain the first two terms of the McLaurin expansion of $\sinh qx$ (the first term is 0). If this is done in the last term of Eq. (22), and then the derivative of the whole equation with respect to y is taken, this for $y = L_2$ can be set equal to zero, since there can be no flux of product towards the outside of

the solid bed, been closed at $y = L_2$:

$$\left(\frac{\partial C_{yp}}{\partial y} \right)_{y=L_2} = 0 = C_{yp}(0) q_{2p} \sinh q_{2p} L_2$$
$$+ C_{yp}'(0) \cosh q_{2p} L_2 - q_r^2 L_2 C_y \tag{24}$$

The last term arises by the differentiation of the integral in Eq. (22) according to Leibniz' rule, after the approximation $\sinh q_{2p} w \approx q_{2p} w$ mentioned before.

So far one is left with Eq. (10), valid for section z and Eq. (24) for section y. To join these equations, the boundary conditions at $z = L_1$ and $y = 0$ are required, which simply are

$$C_{zp}(L_1) = C_{yp}(0) \quad \text{and} \quad a_z D_{zp} \cdot \left(\frac{\partial C_{zp}}{\partial z} \right)_{z=L_1}$$
$$= a_y D_{yp} C_{yp}'(0) \tag{25}$$

The left-hand sides of these relations are both found directly from Eq. (10), and if the results are substituted for $C_{yp}(0)$ and $C_{yp}'(0)$ in Eq. (24), there results

$$C_p(l', p) = \frac{q_r^2 L_2 C_y}{\upsilon} \cdot \left(\frac{q_{2p}}{q_{1p} D_{zp}} \sinh q_{1p} L_1 \cdot \sinh q_{2p} L_2 \right.$$
$$\left. + \frac{a_z}{a_y D_{yp}} \cosh q_{1p} L_1 \cdot \cosh q_{2p} L_2 \right)^{-1} \tag{26}$$

This relation gives the measurable concentration (its t Laplace transform) of the product $C_p(l', p)$ as sampled by the flow reversals in the sampling column from time to time, all quantities inside the parenthesis belonging to the product. Outside there remain q_r^2 defined by Eq. (23), and C_y, which describes the concentration of the reactant in the gas phase in the solid bed region. It was from this quantity that Eq. (1) for the reactant was derived, as described in detail in ref. [16]. The relevant equation there [Eq. (12)] is, for $y = L_2$:

$$C_y = C_y(0) \cosh q_2 L_2 + \frac{C_y'(0)}{q_2} \sinh q_2 L_2 \tag{27}$$

q_2 having been defined as:

$$q_2^2 = \frac{1}{D_y} \cdot \left[p + \frac{k_1 k_R(p + k_2)}{p(p + k_2 + k_R)} \right] \tag{28}$$

Eq. (10) is also valid for the reactant ([16], Eq. (8)):

$$C_z = \frac{\upsilon C(l', p)}{D_z q_1} \sinh q_1 z \tag{29}$$

where $q_1 = \sqrt{p/D_z}$ and this leads us to handle equations for the reactant analogously to Eq. (25), namely:

$$C_z(L_1) = C_y(0) \quad \text{and} \quad a_z D_z \cdot \left(\frac{\partial C_z}{\partial z} \right)_{z=L_1}$$
$$= a_y D_y C_y'(0) \tag{30}$$

The left-hand sides of these relations are obtained directly from Eq. (29), and the results are substituted for $C_y(0)$ and $C'_y(0)$ in Eq. (27), giving.

$$C_y = \frac{\upsilon C(l', p)}{D_z q_1} \cdot \sinh q_1 L_1 \cdot \cosh q_2 L_2$$
$$+ \frac{a_z \upsilon C(l', p)}{a_y D_y q_2} \cdot \cosh q_1 L_1 \cdot \sinh q_2 L_2 \tag{31}$$

This equation must be substituted for C_y in Eq. (26), forming the complete dependence of the product concentration on the time variable. It seems that a very complicated expression will result, and looks rather hopeless to try the inverse Laplace transformation with respect to p of such an expression, so that $c_p(l', t)$ is obtained. The situation, however, may be highly simplified if one approximates the hyperbolic functions $\sinh x$ and $\cosh x$ by transforming their products as previously published [14], and then expand the results in McLaurin series, retaining only the first two terms. More specifically, starting from the products of two hyperbolic functions of Eq. (26) one obtains.

$\sinh q_{1p}L_1 \cdot \sinh q_{2p}L_2$

$$= \frac{1}{2} \left[\cosh(q_{1p}L_1 + q_{2p}L_2) - \cosh(q_{1p}L_1 - q_{2p}L_2) \right]$$
$$\approx \frac{1}{2} \left[1 + \frac{(q_{1p}L_1 + q_{2p}L_2)^2}{2} - 1 \right.$$
$$\left. - \frac{(q_{1p}L_1 - q_{2p}L_2)^2}{2} \right] = q_{1p}L_1 q_{2p}L_2 \tag{32}$$

$\cosh q_{1p}L_1 \cdot \cosh q_{2p}L_2$

$$= \frac{1}{2} \left[\cosh(q_{1p}L_1 + q_{2p}L_2) + \cosh(q_{1p}L_1 - q_{2p}L_2) \right]$$
$$\approx \frac{1}{2} \left[1 + \frac{(q_{1p}L_1 + q_{2p}L_2)^2}{2} + 1 \right.$$
$$\left. + \frac{(q_{1p}L_1 - q_{2p}L_2)^2}{2} \right] = 1 + \frac{(q_{1p}L_1)^2}{2} + \frac{(q_{2p}L_2)^2}{2} \tag{33}$$

In an analogous way, the two hyperbolic functions of Eq. (31) give

$\sinh q_1 L_1 \cdot \cosh q_2 L_2$

$$= \frac{1}{2} \left[\sinh(q_1 L_1 + q_2 L_2) + \sinh(q_1 L_1 - q_2 L_2) \right]$$
$$\approx \frac{1}{2} \left[(q_1 L_1 + q_2 L_2) + (q_1 L_1 - q_2 L_2) \right] = q_1 L_1 \tag{34}$$

$\cosh q_1 L_1 \cdot \sinh q_2 L_2$

$$= \frac{1}{2} \left[\sinh(q_1 L_1 + q_2 L_2) - \sinh(q_1 L_1 - q_2 L_2) \right]$$
$$\approx \frac{1}{2} \left[(q_1 L_1 + q_2 L_2) - (q_1 L_1 - q_2 L_2) \right] = q_2 L_2 \tag{35}$$

Substituting the final results of Eqs. (32) and (33) into Eq. (26), and Eqs. (34) and (35) into (31), to be further used also in (26) for C_y, one finds, after rearrangements

$$C_p(l', p) = C(l', p)\frac{k'}{p(p + k_R + k_2)} \cdot \frac{UT_D}{p + T_D} \tag{36}$$

where $C(l', p)$ is the t transform of the reactant concentration as measured after flow-reversals by its peak heights H as Eq. (1) shows, $C_p(l', p)$ being the respective peak heights H_p of the product measured simultaneously; $k' = k_1 k_2 k_R L_2$ all referring to the reactant; $U = a_y L_1/a_z D_z + L_2/D_y$ referring also to the reactant through its diffusion coefficients D_z and D_y in sections z and y, respectively; and

$$\frac{1}{T_D} = \left(\frac{L_1^2}{2} + \frac{a_y L_1 L_2}{a_z} \right) \cdot \frac{1}{D_{zp}} + \frac{L_2^2}{2D_{yp}} \tag{37}$$

According to Eq. (18) of ref. [16]

$$\frac{C(l', p)}{p(p + k_R + k_2)} = \frac{G}{p^3 + X_1 p^2 + Y_1 p + Z_1} \tag{38}$$

where G has also been defined here by Eq. (2), and X_1, Y_1, Z_1 are given by Eqs. (5)–(7), respectively. Substituting Eq. (38) to Eq. (36), and performing elementary algebra, one obtains

$$C_p(l', p) = \frac{Gk'UT_D}{p^4 + (T_D + X_1)p^3 + (X_1 T_D + Y_1)p^2 + (Y_1 T_D + Z_1)p + Z_1 T_D}$$
$$= \frac{Gk'UT_D}{(p - B_{1p})(p - B_{2p})(p - B_{3p})(p - B_{4p})} \tag{39}$$

where G is given by Eq. (2), k', U, T_D have been defined after Eq. (36), and $B_{1p}, B_{2p}, B_{3p}, B_{4p}$ are the roots of the polynomial in the denominator. According to elementary algebraic knowledge, relations analogous to those of the reactant, i.e., Eqs. (5)–(7) are valid here:

$$T_D + X_1 = -(B_{1p} + B_{2p} + B_{3p} + B_{4p}) = X_2 \tag{40}$$

$$X_1 T_D + Y_1 = B_{1p}B_{2p} + B_{1p}B_{3p} + B_{1p}B_{4p} + B_{2p}B_{3p}$$
$$+ B_{2p}B_{4p} + B_{3p}B_{4p} = Y_2 \tag{41}$$

$$Y_1 T_D + Z_1 = -(B_{1p}B_{2p}B_{3p} + B_{1p}B_{2p}B_{4p} + B_{1p}B_{3p}B_{4p}$$
$$+ B_{2p}B_{3p}B_{4p}) = Z_2 \tag{42}$$

$$Z_1 T_D = B_{1p}B_{2p}B_{3p}B_{4p} = W_2 \tag{43}$$

Taking the p inverse Laplace transformation of Eq. (39), easily found in tables, one has

$$C_p(l', t) = Gk'UT_D \sum_{j=1p}^{4p} A_j \exp(B_j t) \qquad (44)$$

which is analogous in form to Eq. (1) of the reactant, but with four exponential functions of time and A_j been only functions of B_j, e.g.,

$$A_{1p} = [(B_{2p} - B_{1p})(B_{3p} - B_{1p})(B_{4p} - B_{1p})]^{-1} \qquad (45)$$

with analogous expressions for A_{2p}, A_{3p}, and A_{4p} [23]. As before, the sample peak heights are analogous to $C_p(l', t)$ with a proportionality constant g_p, so that

$$H_p^{1/M} = g_p Gk'UT_D \sum_{j=1p}^{4p} A_j \exp(B_j t) \qquad (46)$$

where M is the response factor of the detector, according to its type.

A PC program analogous to that used for calculations based on Eqs. (1)–(7) can be employed for Eqs. (40)–(46), starting from finding A_j and B_j by non-linear least squares fitting of the pairs H_p, t belonging to the product CO_2. It is to be noted that the expression $g_p Gk'UT_D$ in front of the summation is independent of time.

From Eq. (46), it is clear that the only physicochemical information available from fitting the experimental data to the theoretical Eq. (44) comes from the exponential coefficients of time B_j, while the pre-exponential factors A_j are also functions of B_j. This is in contrast with Eq. (4) of the reactant, from which the k value is calculated.

4. Results and discussion

Carbon monoxide dissociation is an important first step in various catalytic processes, such as the methanation reaction, Fisher–Tropsch synthesis etc. The most likely mechanism of CO dissociation is that of the Boudouard (disproportionation) reaction [18,19,24,25]:

$$2CO_{(ads)} \leftrightarrow C_{(ads)} + CO_{2(ads)}$$
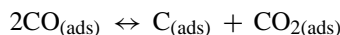
According to Boudouard reaction, adsorbed CO molecules, $CO_{(ads)}$, are dissociated on the catalyst surface, depositing carbon, $C_{(ads)}$, and forming carbon dioxide, $CO_{2(ads)}$. The above mechanism does not exclude the formation of other short-lived indermediate species, such as atomic oxygen, carbonyl species etc. [25]. Carbon monoxide disproportionation can lead to the deposition of carbon at the metal surface. Surface carbon can exist either as carbide-like species, as amorphous carbon or as graphite. Moreover, CO dissociative adsorption can be followed by incorporation into the active metal lattice [25]. These forms of surface carbon exhibit quite differing activities, e.g., carbidic species

can be hydrogenated at relatively low temperatures, whereas graphitic carbon is quite unreactive towards hydrogen. In the present Rh/SiO$_2$ catalyst, it has been found that carbon deposition does not significantly influences the activity towards CO disproportionation [24], and this fact is probably related to the form of the surface deposited carbon.

Two factors are found to affect the dissociation reactions [24]. The first is the electronic factor: it has been found experimentally that the reactivity of transition metals for dissociation decreases from left to right in the periodic table. The reactivity of metals for dissociation reactions is correlated with the metal d band center. The second factor is the geometrical one: both experimental and theoretical studies show that dissociation reactions occur much more efficiently on corrugated surfaces than on flat surfaces.

Rhodium is expected to be very active towards CO dissociation due to the electronic factor. Furthermore, its deposition on a porous solid such as silica combined with the used experimental conditions (high temperatures) result in a corrugated surface. Consequently, a higher dissociation activity due to the geometrical factor is expected for supported Rh/SiO$_2$, especially at higher temperatures.

It is generally assumed that there is a competition between molecular and dissociative adsorption. Molecular adsorption of CO is relatively strong on many noble metal surfaces. Consequently, CO may undergo both dissociative and molecular adsorption on the same surface depending on experimental conditions. It is often observed that molecular adsorption prevails at lower temperatures and dicossiative adsorption occurs at higher temperatures. This pattern may be caused either by kinetics or thermodynamics [24].

Moreover, it is well known in the literature that the equilibrium constant of the Boudouard reaction over noble metals decreases drastically with increasing temperature due to the fact that at low temperatures CO disproportionation is kinetically controlled, while at higher temperatures the equilibrium controls the product composition [24]. Furthermore, mass transfer phenomena often control catalytic processes especially at lower temperatures. It is expected that at lower temperatures mass transfer through the pores of the catalyst should play an important role.

In a recent work, concerning CO dissociation over Rh, Pt and Pt–Rh alloy catalysts [24], it has been also found that: (i) CO adsorption is the rate-determining step, followed by the dissociation step, suggesting a precursor-mediated mechanism for CO dissociative adsorption on the studied catalysts, as well as that (ii) the surface reaction of CO on the catalyst active sites leading to CO dissociation to CO$_2$, follows a first or pseudo first-order step. Thus, the assumption that k_2 value follow a first or pseudo first order is justified (cf. Section 3).

After the short presentation of the main conclusions concerning the CO dissociative adsorption on the studied catalyst [24], the application of mathematical analysis presented in the theoretical section here for both the adsorbate CO and the dissociation product CO$_2$ can be investigated. This investigation is focused on three different temperatures: at a

lower one (200 °C) where CO dissociation activity is slight and mass transfer phenomena may prevail, and at two higher temperatures (300 and 325 °C) in which the disproportionation activity becomes more intense and the kinetic factor becomes more important.

There is a noticeable internal consistency of the theoretical equations derived for the reactant [Eqs. (5)–(7)], and those valid for the product [Eqs. (40)–(43)]. For example, the B_1, B_2, B_3 values calculated from the experimental sample peaks of CO at 300 °C have been found, respectively, 3.65×10^{-2}, 0.428, 0.356 min^{-1}, and the B_{1p}, B_{2p}, B_{3p}, B_{4p} values found from the sample peaks of the product CO_2 in the same experiment were, respectively, 1.43×10^{-2}, 3.47×10^{-2}, 0.418, 0.302 min^{-1}.

It is seen that only the value of (B_{1p}) of CO_2 is somehow different from those of CO, while the B_{2p}, B_{3p}, B_{4p} values differ little (within the calculated standard errors) from the B_1, B_2, B_3 values, respectively, of CO. This is predicted by the theoretical Eq. (40) comparing it with Eq. (5). If one calculates the value of T_D of Eq. (37) using all four possibilities from Eqs. (40)–(43), i.e., using both the B_i values from CO hidden under X_1, Y_1, Z_1, and the B_j values from CO_2 (B_{1p}–B_{4p}), the results obtained are similar, their difference lying within the expected limits of standard errors. A mean diffusion coefficient in the solid bed D_{yp} for CO_2 can be calculated from T_D using Eq. (37), the respective D_y for CO being similar to that of CO_2, as expected owing possibly to a similar adhesion of CO on the surface.

The three rate constants of the theoretical section k_1, k_R, k_2, at three different temperatures have been calculated from the experimental pairs H, t, by means of the two PC programs listed in Appendices A and B. They are collected in Table 1, together with the D_y and D_{yp} values. It should be noted that it is difficult to estimate the errors of the physicochemical parameters mentioned in Table 1, since they emerge from a series of a rather complex calculations and the application of the rule of propagation of errors in a long sequence of steps does not give reliable final errors. The following conclusions can be derived from the rate constants of Table 1:

The values of the calculated CO adsorption rate constants, k_1, are lower than the respective adsorption/desorption, k_R, and surface reaction rate constants, k_2, in agreement with the results of previous studies [24] that CO adsorption is the slow rate-determining step of the overall dissociation process. Adsorption rate constant values increase with increasing temperature. Thus, carbon monoxide adsorption is a temperature-activated process. The respective mean activation energy is calculated by means of the Arrhenius equation equal to 61.0 kJ mol^{-1}, which is indicative of chemisorption. Carbon monoxide adsorption rates drastically increase at temperatures higher than 300 °C, in close agreement with the observed disproportionation activity [24].

The adsorption/desorption rate constant values, k_R, decrease with increasing temperature.

Dissociation rate constant values, k_2, pass through a maximum at 300 °C. This anomalous behavior of k_2 values, in contrast with the fact that dissociation reaction is expected to be an activated process, can be explained by assuming that the calculated rate constants for the dissociation of CO, k_2, are apparent ones. These are related to the true values via the equation: $k_{2(true)} = k_2/K_{BR}$, where K_{BR} is the equilibrium constant for the Boudouard reaction. It is well known in the literature that the equilibrium constant of the Boudouard reaction, K_{BR}, over noble metals decreases drastically with increasing temperature due to the fact that at low temperatures CO disproportionation is kinetically controlled while at higher temperatures the equilibrium controls the product composition. Thus, a small decrease of the k_2 value versus temperature, accompanied by a higher decrease of the equilibrium constant K, leads to an in increase in the $k_{2(true)}$ value with temperature [24].

Total diffusion coefficients in the solid bed for the adsorbate CO, D_y, and for the dissociation product CO_2, D_{yp}, exhibit a behavior similar to that of k_1 and k_2 values, respectively. Bearing in mind that surface diffusion is ordinarily an activation process much like liquid diffusion; its activation energy is expected to be a small fraction of the heat of adsorption. Thus, the mean activation energy value for CO, calculated by means of the Arrhenius equation, is only 7.1 kJ mol^{-1}, which is much lower than that of the adsorption ($\approx$61.0 kJ mol^{-1}).

In porous heterogeneous catalysts diffusion phenomena are probably more important than activation energies, as expressed by the Thiele-type modulus group Φ_s (dimensionless), which for spherical pellets of radius r_s is given by the relation [26]

$$\Phi_s = \frac{r_s}{3}\sqrt{\frac{k\rho}{D_e}} \quad (47)$$

where k (s^{-1} cm^3 g^{-1}) is the conventional reaction rate constant, ρ (g cm^{-3}) the density of the solid and D_e (cm^2 s^{-1}) the effective diffusion coefficient of the gases in the catalytic bed.

Eq. (47) is based on two physicochemical quantities, which are difficult to determine or calculate experimentally, i.e., the k and D_e, especially the second. This is usually found from the relation

$$D_e = \frac{\varepsilon_M^2}{(1/D_g) + (1/D_k)} \quad (48)$$

where D_g is the diffusion coefficient of the reactant in the gas phase and D_k the respective Knudsen diffusion coefficient, with ε_M the macroporous void fraction in the bed.

For such small particles as those in the present work ($r_s = 5 \times 10^{-3}$ cm), the effectiveness factor η of the catalytic bed, as calculated [26] by the relation

$$\eta = \frac{1}{\Phi_s}\left(\frac{1}{\tanh 3\Phi_s} - \frac{1}{3\Phi_s}\right) \quad (49)$$

is expected to be unity.

Table 2
Thiele-type modulus Φ_s and effectiveness factor η for the adsorbate CO and the product of CO disproportionation CO_2

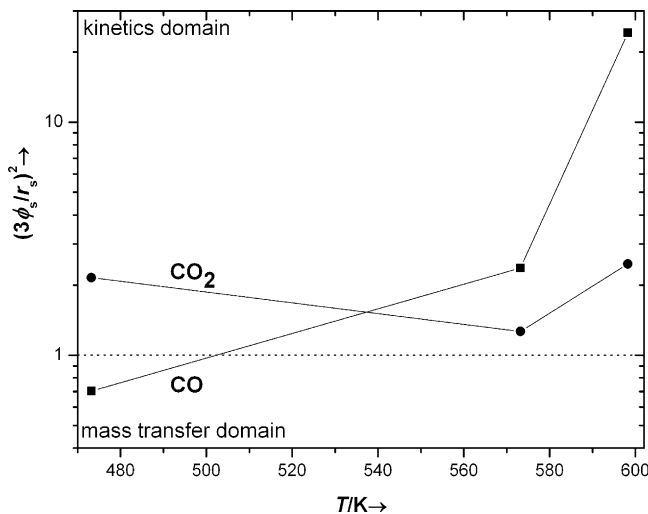| T (K)	Carbon monoxide		Carbon dioxide	
	$10^3 \times \Phi_s$	η	$10^3 \times \Phi_s$	η
473.2	1.400	0.9999	7.735	0.9999
573.2	2.566	0.9999	5.924	0.9999
598.2	8.193	0.9999	8.282	0.9999

Fig. 1. Temperature variation of the Thiele-type modulus $(3\Phi_s/r_s)^2$ for the adsorbate carbon monoxide and its dissociation product carbon dioxide, in a semi-logarithmic plot.

The Φ_s provides a measure of the competition between kinetics and mass-transfer phenomena, over porous solids. At the limiting case where: $(3\Phi_s/r_s)^2 = k\rho/D_e = 1$, the kinetic and the mass-transfer factors become equivalent, while when: $(3\Phi_s/r_s)^2 > 1$, the kinetic factor $(k\rho)$ prevails and vice-versa. Here, it can be assumed that $k\rho = k_1$, in the case of the adsorbate (CO), since CO adsorption is the rate-determining step of CO disproportionation [24], while $k\rho = k_2$, in the case of the product of dissociation (CO_2), and $D_e = D_y$ or

D_{yp}, i.e., the effective diffusivities in $cm^2\ s^{-1}$ of the gaseous reactant or product in the catalyst bed found as previously described.

Using the values listed in Table 1 found from experimental data, one can calculate Φ_s from Eq. (47), and from that the effectiveness factor η of the catalyst by the Eq. (49). The results found by the PC programs of the Appendices A and B are listed in Table 2 and the temperature variation of the Thiele-type modulus group Φ_s is shown in Fig. 1.

An ideal experimental value effectiveness factor η of the catalytic bed, at the temperatures studied is found by the method described here, using both the reactant and product chromatographic peaks.

The results concerning Φ_s show that in the case of carbon monoxide there is a critical temperature ($\approx$500 K) below which mass-transfer is more important than kinetics; the latter prevail at temperatures higher than 500 K. In the case of the dissociation product (CO_2) kinetics prevail in the whole studied temperature range. These are important new findings of the presented methodology, concerning the mechanism of carbon monoxide dissociation over the studied Rh/SiO_2 catalyst. By using the presented GC methodology, the question which of the two processes, mass-transfer or kinetics, is more important in a particular temperature can be directly answered, while in conventional heterogeneous catalysis studies the competition is usually indirectly investigated from the temperature variation of the catalytic activity. Moreover, the presented methodology takes also into account the possible product of the adsorbate–adsorbent interaction. Furthermore, the methodology presented in this work can be applied not only for solid catalysts, but also generally for solids of chromatographic interest.

Appendix A. GW-Basic Program for the calculation of A_j and B_j of Eq. (44) pertaining to the product

```
10 REM Calculation of Exponential Functions for the Product
20 REM Non-Linear Regression Analysis of Product
30 REM HP^(1/M)=A1P*EXP(B1P*T)+S*A2P*EXP(B2P*T)+P*A3P*EXP(B3P*T)+X*A4P*EXP(B4P*T)
40 REM H^(1/M)=A1*EXP(B1*T)+S*A2*EXP(B2*T)+P*A3*EXP(B3)
50 REM N2    = Minimum number of points of first exponential function
60 REM MAX   = Square of maximum correlation coefficient
70 REM OPT   = Final optional choice of variables when OPT=1
80 REM J     = Number of points of first exponential function
90 REM G     = Number of points of second exponential function
100 REM F    = Number of points of third exponential function
110 REM K,L  = First and last point of linear regression in subroutine
120 REM SA,SB = Standard errors of A and B in each linear regression
130 REM Y(I)  = Ordinate for each linear regression in the subroutine
140 REM D(I)= Function for calculating the squared correlation coefficient
150 CLEAR ,,10000
160 INPUT "Maximum number of pairs of product H,T=";NA
170 INPUT "Minimum number of pairs of product H,T=";NS
180 DIM T(2*NA),H(2*NA),Y(2*NA),U(2*NA),D(2*NA)
190 INPUT "Response Factor of the Detector M=";M
200 INPUT "Length L1 of Section z(cm)=";L1
210 L1=70
220 INPUT "Length L2 of Section y(cm)=";L2
230 INPUT "External Porosity E of the Solid Bed =";E
240 INPUT "Cross Sectional Area Az(cm^2) of Empty Section L1=";AZ
250 INPUT "Cross Sectional Area Ay(cm^2) of Filled Section L2=";AY
260 INPUT "Amount of Adsorbent per Unit Length of Bed As(g/cm)=";AS
270 INPUT "Volumetric Flow Rate of Carrier Gas V'(cm^3/min)=";V0
280 INPUT "Negative Diffusion Coefficient of Product (cm^2/s)=";D1P
290   FOR I=1 TO NA
300    READ T(I), H(I)
310   NEXT I
320 MAX=0:OPT=0
330 FOR N=NA TO NS STEP-1
340 N2=INT(N/7+.5)
```

```
350 REM Calculation of A1P and B1P with H,T pairs ranging from N2 to N-2*N2-3
360 FOR J=N2 TO N-2*N2-3
370    K=N-J+1
380    L=N
390    FOR I=K TO L
400       Y(I)=(1/M)*LOG(H(I))
410    NEXT I
420    GOSUB 4000     :REM Subroutine for linear regression analysis
430    A1P=EXP(A)
440    B1P=B
450    SA1P=SA
460    SB1P=SB
470    IF OPT=1 THEN  510
480 REM Calculation of A2P and B2P with H,T pairs ranging from N2 to N-J-N2-3 with both prefixes -1 or +1
490    FOR S=-1 TO +1 STEP 2
500       FOR G=N2 TO N-J-N2-3
510          K=N-J-G+1
520          L=N-J
530          FOR I=K TO L
540             U(I)=S*H(I)^(1/M)-S*A1P*EXP(B1P*T(I))
550             Y(I)=LOG(ABS(U(I)))
560          NEXT I
570          GOSUB 4000 :REM Subroutine for linear regression analysis
580          A2P=EXP(A)
590          B2P=B
600          SA2P=SA
610          SB2P=SB
620          IF OPT=1 THEN 660
630 REM Calculation of A3P and B3P with H,T pairs ranging from N2 to N-J-G-3 with both prefixes -1 or +1
640             FOR P=-1 TO +1 STEP 2
650                FOR F=N2 TO N-J-G-3
660                   K=N-J-G-F+1
670                   L=N-J-G
680                   FOR I=K TO L
690                      U(I)=P*(H(I)^(1/M)-A1P*EXP(B1P*T(I))-S*A2P*EXP(B2P*T(I)))
700                      Y(I)=LOG(ABS(U(I)))
710                   NEXT I
720                GOSUB 4000:REM Subroutine for linear regression analysis
730                   A3P=EXP(A)
```

```
740        B3P=B

750        SA3P=SA

760        SB3P=SB

770        IF OPT=1 THEN 800

780 REM Calculation of A4P and B4P with H,T pairs ranging from 1 to N-J-G-F  with both prefixes -1 or +1

790        FOR X=-1 TO +1 STEP 2

800        K=1

810        L=N-J-G-F

820        FOR I=K TO L

830 U(I)=X*(H(I)^(1/M)-A1P*EXP(B1P*T(I))-S*A2P*EXP(B2P*T(I))-P*A3P*EXP(B3P*T(I)))

840            Y(I)=LOG(ABS(U(I)))

850        NEXT I

860      GOSUB 4000  :REM Subroutine for linear regression analysis

870        A4P=EXP(A)

880        B4P=B

890        SA4P=SA

900        SB4P=SB

910        IF OPT=1 THEN 1140

920        C1=0

930        C2=0

940        C3=0

950        FOR I=1 TO N

960                D(I)=H(I)^(1/M)-A1P*EXP(B1P*T(I))-S*A2P*EXP(B2P*T(I))-P*A3P*EXP(B3P*T(I))-
X*A4P*EXP(B4P*T(I))

970            C1=C1+D(I)^2

980            C2=C2+H(I)^(2/M)

990            C3=C3+H(I)^(1/M)

1000           NEXT I

1010        R=1-C1/(C2-C3^2/N)

1020 IF R>MAX THEN MAX=R:SMAX=S:PMAX=P:XMAX=X:JMAX=J:GMAX=G:FMAX=F:NMAX=N

1030 PRINT MAX

1040          NEXT X

1050        NEXT F

1060      NEXT P

1070     NEXT G

1080   NEXT S

1090 NEXT J

1100 NEXT N

1110 S=SMAX:P=PMAX:X=XMAX:J=JMAX:G=GMAX:F=FMAX:N=NMAX:OPT=1
```

```
1120 GOTO 370
1130 LPRINT
1140 LPRINT "Intercept Ln(A1P) and its Standard error =";LOG(A1P) "+-"SA1P
1150 LPRINT "Slope B1P and its Standard error=";B1P "+-"SB1P
1160 LPRINT
1170 LPRINT "Intercept Ln(A2P) and its Standard error=";LOG(A2P) "+-"SA2P
1180 LPRINT "Slope B2P and its Standard error=";B2P "+-"SB2P
1190 LPRINT
1200 LPRINT "Intercept Ln(A3P) and its Standard error=";LOG(A3P) "+-"SA3P
1210 LPRINT "Slope B3P and its Standard error=";B3P "+-"SB3P
1220 LPRINT
1230 LPRINT "Intercept Ln(A4P) and its Standard error=";LOG(A4P) "+-"SA4P
1240 LPRINT "Slope B4P and its Standard error=";B4P "+-"SB4P
1250 LPRINT
1260 LPRINT "Square of maximum correlation coefficient r^2=";MAX
1270 LPRINT "Optimum values of N of product=";NMAX
1280 LPRINT "Optimum numbers of points for 1st, 2nd,3rd,4th exponential
functions,respectively=";JMAX","GMAX","FMAX"and"N-JMAX-GMAX-FMAX
1290 LPRINT "Values of S,P and X,respectively ="; SMAX","PMAX"and"XMAX
1300 LPRINT
1310 X2=-(B1P+B2P+B3P+B4P)
1320 LPRINT "Value of X2=-(B1p+B2p+B3p+B4p) in 1/min=";X2
1330 END
4000  REM Linear regression of Y(I) = A + B T(I)
4010 S1=0
4020 S2=0
4030 S3=0
4040 S4=0
4050 S5=0
4060   FOR I=K TO L
4070   S1=S1+T(I)
4080   S2=S2+T(I)^2
4090   S3=S3+Y(I)
4100   S4=S4+Y(I)^2
4110   S5=S5+T(I)*Y(I)
4120 NEXT I
4130 Z=L-K+1  :REM Number of points for the linear regression analysis
4140 M1=S5-S1*S3/Z
4150 M2=S2-S1^2/Z

4160 M3=S4-S3^2/Z
4170 A=(S3-S1*M1/M2)/Z
4180 B=M1/M2
4190 SYT=SQR(ABS(S4-A*S3-B*S5)/(Z-2))
4200 SA=SYT*SQR(S2/Z/M2)
4210 SB=SYT/SQR(M2)
4220 RETURN
```

Appendix B. GW-Basic program for the calculation of A_i and B_i of Eq. (1)b pertaining to reactant, and of physicochemical quantities k_1, k_R, k_2, D_y, D_{yp}, Φ_s and η.

```
10 REM Calculations for the Reactant Adsorbed on Heterogeneous Surfaces
20 REM Non-Linear Regression Analysis of Function:
30 REM H^(1/M)=A1*EXP(B1*T)+S*A2*EXP(B2*T)+P*A3*EXP(B3*T)
40 REM N2    = Minimum number of points of first exponential function
50 REM MAX   = Square of maximum correlation coefficient
60 REM OPT   = Final optional choice of variables when OPT=1
70 REM J     = Number of points of first exponential function
80 REM G     = Number of points of second exponential function
90 REM F     = Number of points of third exponential function
100 REM SA,SB = Standard errors of A and B in each linear regression
110 REM Y(I) = Ordinate for each linear regression in the subroutine
120 REM U(I)= Variable remaining by  removal of the previous one,or two exponential functions
130 REM D(I)= Function for calculating the squared correlation coefficient
140 CLEAR ,,10000
150 INPUT "Maximum number of pairs H,T=";NF
160 INPUT "Minimum number of pairs H,T=";NS
170 DIM T(NF),H(NF),Y(NF),U(NF),D(NF)
180 INPUT "Response factor=";M
190 INPUT "Temperature in K=";T0
200 INPUT "Lenth L1(cm) of Section z=";L1
210 INPUT "Length L2(cm) of Section y=";L2
220 INPUT "External Porosity E of the Solid bed=";E
230 INPUT "Cross sectional area Az(cm^2) of Empty Section L1 =";AZ
240 INPUT "Cross Sectional Area Ay(cm^2) of Filled Section L2=";AY
250 INPUT "Amount of Adsorbent per Unit Length of Bed AS(g/cm)=";AS
260 INPUT "Volumetric Flow-rate of Carrier Gas V'(cm^3/min)=";V0
270 INPUT "Negative Diffusion Coefficient of Gaseous Reactant (cm^2/s)=";D1
280 INPUT "Negative Diffusion Coefficient of Product in the Gas(cm^2/s)=";D1P
290 INPUT "Amount of Reactant injected NB(mol)=";NB
300 INPUT "Sum of -(B1p+B2p+B3p+B4p)=X2 for the product=";X2
310 INPUT "Radius of Catalyst Particle (cm)=";RS
320   FOR I=1 TO NF
330    READ T(I), H(I)
340   NEXT I
```

```
350 MAX=0:OPT=0
360 FOR N=NF TO NS STEP -1
370 N2=INT(N/6+.5)
380  REM Calculation of A1 and B1 with H,T pairs ranging from N2 to N-N2-3
390 FOR J=N2 TO N-N2-3
400    K=N-J+1
410    L=N
420    FOR I=K TO L
430      Y(I)=(1/M)*LOG(H(I))
440    NEXT I
450    GOSUB 4000      : REM Subroutine for linear regression analysis
460    A1=EXP(A)
470    B1=B
480    SA1=SA
490    SB1=SB
500    IF OPT=1 THEN  540
510  REM Calculation of A2 and B2 with H,T pairs ranging from N2 to N-J-3 and both prefixes -1 and +1
520    FOR S=-1 TO +1  STEP 2
530      FOR G=N2 TO N-J-3
540        K=N-J-G+1
550        L=N-J
560        FOR I=K TO L
570          U(I)=S*H(I)^(1/M)-S*A1*EXP(B1*T(I))
580          Y(I)=LOG(ABS(U(I)))
590        NEXT I
600        GOSUB 4000    : REM Subroutine for linear regression analysis
610        A2=EXP(A)
620        B2=B
630        SA2=SA
640        SB2=SB
650        IF OPT=1 THEN 680
660  REM Calculation of A3 and B3 with H,T pairs ranging from 1 to N-J-G, with both prefixes -1 and +1
670          FOR P=-1 TO +1 STEP 2
680            K=1
690            L=N-J-G
700            FOR I=K TO L
710              U(I)=P*(H(I)^(1/M)-A1*EXP(B1*T(I))-S*A2*EXP(B2*T(I)))
720              Y(I)=LOG(ABS(U(I)))
730            NEXT I
```

740   **GOSUB 4000 : REM Subroutine for linear regression analysis**

750   **A3=EXP(A)**

760   **B3=B**

770   **SA3=SA**

780   **SB3=SB**

790   **IF OPT=1 THEN 990**

800   **C1=0**

810   **C2=0**

820   **C3=0**

830   **FOR I=1 TO N**

840   **D(I)=H(I)^(1/M)-A1*EXP(B1*T(I))-S*A2*EXP(B2*T(I))-P*A3*EXP(B3*T(I))**

850   **C1=C1+D(I)^2**

860   **C2=C2+H(I)^(2/M)**

870   **C3=C3+H(I)^(1/M)**

880   **NEXT 1**

890   **R=1-C1/(C2-C3^2/N)**

900   **IF R>MAX THEN MAX=R:SMAX=S:PMAX=P:JMAX=J:GMAX=G:NMAX=N**

910 PRINT MAX

920   **NEXT P**

930   **NEXT G**

940 **NEXT S**

950 NEXT J

960 NEXT N

970 S=SMAX:P=PMAX:J=JMAX:G=GMAX:N=NMAX:OPT=1

980 GOTO 400

990 LPRINT "Intercept Ln(A1) and its Standard error=";LOG(A1) "+-"SA1

1000 LPRINT "Slope B1 and its Standard error=";B1 "+-"SB1

1010 LPRINT

1020 LPRINT "Intercept Ln(A2) and its Standard error=";LOG(A2) "+-"SA2

1030 LPRINT "Slope B2 and its Standard error=";B2 "+-"SB2

1040 LPRINT

1050 LPRINT "Intercept Ln(A3) and its Standard error=";LOG(A3) "+-"SA3

1060 LPRINT "Slope B3 and its Standard error=";B3 "+-"SB3

1070 LPRINT

1080 LPRINT "Square of maximum correlation coefficient r^2=";MAX

1090 LPRINT "Optimum value of pairs N=";NMAX

1100 LPRINT "Optimum values of points for 1st, 2nd and 3rd exponential functions ,respectively=";JMAX","GMAX"and"N-JMAX-GMAX

1110 LPRINT "Values of S and P, respectively =";SMAX"and"PMAX

```
1120 LPRINT
1130 REM Enter DATA in lines 3000-3040 in the order H(peak height), T(min)
1140 A1B=A1*(B1-B2)*(B1-B3)
1150 A2B=A2*(B2-B1)*(B2-B3)
1160 A3B=A3*(B3-B1)*(B3-B2)
1170 A31=A3B/A1B:A21=A2B/A1B
1180 K31=(B3^2-A31*B1^2)/(A31*B1-B3)
1190 K21=(B2^2-A21*B1^2)/(A21*B1-B2)
1200 KAV=(K31+K21)/2
1210 X1=-(B1+B2+B3)
1220 Y1=(B1*B2+B1*B3+B2*B3)
1230 Z1=-(B1*B2*B3)
1240 AA1=2*D1*60/L1^2
1250 Q2=2*L2*AY*E/AZ/L1
1260 INVAA2=1/(X1-KAV)-(1+Q2)/AA1:AA2=1/INVAA2
1270 D2=AA2*L2^2/2
1280 TD=X2-X1
1290 INVAA2P=1/TD-(L1^2/2+AY*L1*L2/AZ)/(D1P*60)
1300 AA2P=1/INVAA2P
1310 D2P=L2^2*AA2P/2
1320 AQ1=AA1+AA2*Q2:AQ2=AA1+AA2+AA2*Q2
1330 K1KR=(Y1*AQ2-AA1*AA2*KAV)/AQ1
1340 K1K2KR=Z1*AQ2/AQ1
1350 K2=K1K2KR/K1KR
1360 KR=KAV-K2
1370 K1=K1KR/KR
1380 LPRINT "Coefficient for Isotherm Integration k1 in 1/s=";K1/60
1385 LPRINT
1390 LPRINT "Adsorption/Desorption Rate Constant kR in 1/s=";KR/60
1395 LPRINT
1400 LPRINT "Surface Reaction Rate Constant k2 in 1/s=";K2/60
1410 LPRINT
1420 LPRINT "Total Reactant Diffusion Coefficient in Bed Dy(cm^2/s)=";D2/60
1430 LPRINT
1440 LPRINT "Total Product Diffusion Coefficient in Bed Dyp(cm^2/s)=";D2P/60
1450 A=A1/B1+A2/B2+A3/B3
1460 G1=ABS(V0*A/NB)
1470 LPRINT
1480 LPRINT "Calibration Factor of Detector g in cm per mol/cm^3=";G1
```

```
1490 LPRINT
1500 FSDY=RS*SQR(K2/D2)/3
1510 TANHDY=(EXP(3*FSDY)-EXP(-3*FSDY))/(EXP(3*FSDY)+EXP(-3*FSDY))
1520 HTADY=(1/TANHDY-1/3/FSDY)/FSDY
1530 LPRINT "Thiele-type Modulus Fs(Dimensionless) Based on Dy=";FSDY
1540 LPRINT "Effectiveness Factor n (dimensionless) Based on Dy";HTADY
1550 FSDYP=RS*SQR(K2/D2P)/3
1560 TANHDYP=(EXP(3*FSDYP)-EXP(-3*FSDYP))/(EXP(3*FSDYP)+EXP(-3*FSDYP))
1570 HTADYP=(1/TANHDYP-1/3/FSDYP)/FSDYP
1580 LPRINT "Thiele-type Modulus Fsp(Dimensionless) Based on Dyp=";FSDYP
1590 LPRINT "Effectiveness Factor n (dimensionless) Based on Dyp=";HTADYP
1600 END
4000  REM Linear regression of Y(I) = A + B T(I)
4010 S1=0
4020 S2=0
4030 S3=0
4040 S4=0
4050 S5=0
4060   FOR I=K TO L
4070   S1=S1+T(I)
4080   S2=S2+T(I)^2
4090   S3=S3+Y(I)
4100   S4=S4+Y(I)^2
4110   S5=S5+T(I)*Y(I)
4120 NEXT I
4130 Z=L-K+1  :REM Number of points for the linear regression analysis
4140 M1=S5-S1*S3/Z
4150 M2=S2-S1^2/Z
4160 M3=S4-S3^2/Z
4170 A=(S3-S1*M1/M2)/Z
4180 B=M1/M2
4190 SYT=SQR(ABS(S4-A*S3-B*S5)/(Z-2))
4200 SA=SYT*SQR(S2/Z/M2)
4210 SB=SYT/SQR(M2)
4220 RETURN
```

References

[1] D.W. Bassett, H.W. Habgood, J. Phys. Chem. 64 (1960) 769.

[2] N.A. Katsanos, J. Chromatogr. A 1037 (2004) 125.

[3] M. Czok, G. Guiochon, Anal. Chem. 62 (1990) 189.

[4] J.R. Conder, C.L. Young, Physicochemical Measurements by Gas Chromatography, Wiley, Chichester, 1979.

[5] C.S.G. Phillips, A.J. Hart-Davies, R.G.L. Saul, J. Wormald, J. Gas Chromatogr. 5 (1967) 424.

[6] G. Karaiskakis, N.A. Katsanos, I. Georgiadou, A. Lycourghiotis, J. Chem. Soc., Faraday Trans. 1 78 (1982) 2017.

[7] M. Kotinopoulos, G. Karaiskakis, N.A. Katsanos, J. Chem. Soc., Faraday Trans. 1 78 (1982) 3379.

[8] N.A. Katsanos, M. Kotinopoulos, J. Chem. Soc., Faraday Trans. 1 81 (1985) 951.

[9] N.A. Katsanos, G. Karaiskakis, A. Niotis, J. Catal. 94 (1985) 376.

[10] E. Dalas, N.A. Katsanos, G. Karaiskakis, J. Chem. Soc., Faraday Trans. 1 82 (1986) 2897.

[11] N.A. Katsanos, Catal. Today 2 (1988) 605.

[12] N.A. Katsanos, E. Arvanitopoulou, F. Roubani-Kalantzopoulou, A. Kalantzopoulos, J. Phys. Chem. B 103 (1999) 1152.

[13] N.A. Katsanos, E. Iliopoulou, F. Roubani-Kalantzopoulou, E. Kalogirou, J. Phys. Chem. B. 103 (1999) 10228.

[14] N.A. Katsanos, D. Gavril, G. Karaiskakis, J. Chromatogr. A 983 (2003) 177.

[15] N.A. Katsanos, F. Roubani-Kalantzopoulou, E. Iliopoulou, I. Bassiotis, V. Siokos, M.N. Vrahatis, V.P. Plagianakos, Colloid Surf. A 201 (2002) 173.

[16] N. Bakaoukas, A. Koliadima, L. Farmakis, G. Karaiskakis, N.A. Katsanos, Chromatographia 57 (2003) 783.

[17] S. Margariti, N.A. Katsanos, F. Roubani-Kalantzopoulou, Colloid Surf. A 226 (2003) 55.

[18] N.A. Katsanos, R. Thede, F. Roubani-Kalantzopoulou, J. Chromatogr. A 795 (1998) 133.

[19] N.A. Katsanos, F. Roubani-Kalantzopoulou, Adv. Chromatogr. 40 (2000) 231.

[20] N.A. Katsanos, J. Chromatogr. A 969 (2002) 3.

[21] N.A. Katsanos, D. Gavril, J. Kapolos, G. Karaiskakis, J. Colloid Interface Sci. 270 (2003) 455.

[22] Ch. Abatzoglou, E. Iliopoulou, N.A. Katsanos, F. Roubani-Kalantzopoulou, J. Chromatogr. A 775 (1997) 211.

[23] F. Oberhettinger, L. Badii, Tables of Laplace Transforms, Springer, Berlin, 1973, p. 218.

[24] D. Gavril, V. Loukopoulos, G. Karaiskakis, Chromatographia 59 (2004) 721.

[25] M. Maciejewski, A. Baiker, J. Phys. Chem. 98 (1994) 285.

[26] J.M. Smith, Chemical Engineering Kinetics, third edn., McGraw-Hill, New York, 1981, p. 479.